Theor Appl Climatol (2017) 127:551–561
DOI 10.1007/s00704-015-1649-x

ORIGINAL PAPER

# Impact of East Asian winter monsoon on MJO over the equatorial western Pacific

Xiong Chen[1] · Chongyin Li[1,2] · Jian Ling[2] · Yanke Tan[1]

Received: 6 January 2015 / Accepted: 24 September 2015 / Published online: 9 October 2015


**Abstract** This paper investigates the processes and mechanisms by which the East Asian winter monsoon (EAWM) affects the Madden-Julian oscillation (MJO) over the equatorial western Pacific in boreal winter (November–April). The results show that both the EAWM and MJO over the equatorial western Pacific have prominent interannual and interdecadal variabilities, and they are closely related, especially on the interannual timescales. The EAWM influences MJO via the feedback effect of convective heating, because the strong northerlies of EAWM can enhance the ascending motion and lead the convection to be strengthened over the equatorial western Pacific by reinforcing the convergence in the lower troposphere. Daily composite analysis in the phase 4 of MJO (i.e., strong MJO convection over the Maritime Continent and equatorial western Pacific) shows that the kinetic energy, outgoing longwave radiation (OLR), moisture flux, vertical velocity, zonal wind, moist static energy, and atmospheric stability differ greatly between strong and weak EAWM processes over the western Pacific. The strong EAWM causes the intensity of MJO to increase, and the eastward propagation of MJO to become more persistent. MJO activities over the equatorial western Pacific have different modes. Furthermore, these modes have differing relationships with the EAWM, and other factors can also affect the activities of MJO; consequently, the relationship between the MJO and EAWM shows both interannual and interdecadal variabilities.

✉ Jian Ling
lingjian@lasg.iap.ac.cn

Xiong Chen
cx3212007753@163.com

[1] College of Meteorology and Oceanography, PLA University of Science and Technology, Nanjing 211101, China

[2] LASG, Institute of Atmospheric Physics, CAS, Beijing 100029, China

## 1 Introduction

The East Asian winter monsoon (EAWM) HuangHuangis one of the most active atmospheric circulation systems in the boreal winter. It not only affects the weather and climate over the East Asia but can also modify the variations of tropical atmosphere and ocean. The EAWM also plays an important role in the global weather and climate anomalies (Chang et al. 1979; Chan and Li 2004; Huang et al. 2007a; Yan et al. 2009; Zhou 2011). Consequently, the EAWM is one of the most important issues facing researchers, especially Chinese scholars, and a good understanding of its activities and variability has been developed. In recent years, an increasing attention has focused on the anomalies of EAWM, such as the interaction between the EAWM and ENSO (Li and Mu 2000; Zhou et al. 2007), the characteristics of EAWM variability and its mechanism (Huang et al. 2003; Wang and Ding 2006), and the relationship between the EAWM and the activities of quasi-stationary planetary wave (Chen et al. 2005; Huang et al. 2007b; Wang et al. 2009).

Madden-Julian oscillation (MJO) first discovered by Madden and Julian (1971, 1972) is characterized with a period about 30–60 days. Most of the researches have shown that MJO has a significant impact on the global weather and climate and is closely related to the anomalous weather and climate in many areas (Madden and Julian 1994; Zhang 2005, 2013; Li et al. 2014). For example, MJO activities in boreal summer are directly related to the outbreak and interruption of the East Asian summer monsoon and its precipitation (Yang and Li 2003; Zhou and Chan 2005; Lü et al. 2012). MJO activities are also closely related to the ENSO cycle. The

MJO over the equatorial western Pacific strengthens significantly in the winter and spring prior to El Niño occurrence but decreases rapidly during the mature stage of El Niño (Li and Zhou 1994; Zhang and Gottschalck 2002; Hendon et al. 2007). Furthermore, the MJO also influences the formation and activities of the typhoon over the western Pacific (Zhu et al. 2004; Pan et al. 2010; Li et al. 2012, Li and Zhou 2013a, 2013b).The importance of extratropical influences on the initiation and maintenance of the MJO has been argued using reanalysis data and numerical analysis for a long time (Liebmann and Hartmann 1984; Murakami 1988; Hsu et al. 1990; Ray et al. 2009, Ray and Zhang 2010; Ling et al. 2013, 2014). Wang et al. (2012) studied a case in which a northerly surge reinforced MJO over the Indian Ocean during its initiation phase and found that such subtropical cold surges are likely to strengthen and accelerate the buildup of deep MJO convection during the initiation phase of MJO. The latitudinal transport of momentum from the extratropics is crucial to the generation of westerly associated with the MJO initiation in the lower troposphere in the tropics (Ray et al. 2009; Ray and Zhang 2010).

Many studies have shown that the strong EAWM can enhance the convection over the South China Sea and tropical western Pacific and lead to an anomalous cyclonic circulation to the east of the Philippines (Chang et al. 1979; Ji et al. 1997). However, the feedback effect of convective heating is one of the main mechanisms for the initiation and maintenance of MJO (Li 1985; Lau and Peng 1987; Li et al. 2009), which means that the EAWM is closely related to the variation of the MJO over the equatorial western Pacific. In the late 1980s, Li (1989) pointed out that the persistent and strong northerly of EAWM can promote the occurrence of El Niño event, as it can strengthen the anomalous westerly and the 30–60 days oscillation in the atmosphere over the western Pacific by reinforcing convection there. However, the processes and mechanisms by which the EAWM affects the MJO over the equatorial western Pacific remain unclear. Therefore, this study aims to further investigate these processes and mechanisms using reanalysis data.

The remainder of this paper is organized as follows. The data and methods are described briefly in section 2. The relationship between the EAWM and MJO and the processes by which the EAWM impacts the MJO are analyzed in section 3. A further study of these influences and mechanisms in the phase 4 of MJO is provided in section 4 using composite analysis. Finally, the summary and discussion are provided in section 5.

## 2 Data and methods

The daily mean atmospheric data are from the National Centers for Environmental Prediction/National Center for Atmospheric Research (NCEP/NCAR) (Kalnay et al. 1996), including wind, relative humidity covering the period from 1 January 1948 to 31 December 2011 with a horizontal resolution of 2.5° × 2.5°. The daily mean outgoing longwave radiation (OLR) data with a horizontal resolution of 2.5° × 2.5° are from the National Oceanic and Atmospheric Administration (NOAA) (Liebmann and Smith 1996) from 1 January 1975 to 31 December 2011. The real-time multivariate MJO (RMM) index developed by Wheeler and Hendon (2004) is from the Australian Bureau of Meteorology.

The main methods used in this study were composite and correlation analyses. The anomalies were generated by removing the annual cycle. The MJO signal was obtained by using the 30–60 days Lanczos bandpass filter with a 200-point window (Duchon 1979).

## 3 Relationship between the MJO and EAWM

### 3.1 Correlation of the MJO and EAWM

The strength of the EAWM can be represented by the EAWM index. The EAWM index defined by meridional wind in the lower troposphere can better reflect the impact of the EAWM on the tropical atmosphere and ocean (Wang and Chen 2010). Here, the EAWM index is defined as the meridional wind averaged over 10°–30° N, 115°–130° E at 1000 hPa (Ji et al. 1997). Therefore, a higher/lower index value indicates a weaker/stronger EAWM. The intensity of MJO is represented by the MJO kinetic energy at 850 hPa (Li and Zhou 1994), and the MJO intensity index is defined as the MJO kinetic energy at 850 hPa averaged over the equatorial western Pacific (10° S–10° N, 120°–150° E).

The normalized EAWM and MJO indices in boreal winter from 1948 to 2010 (Fig. 1) clearly show the pronounced interannual and interdecadal variabilities of them, as well as the obviously out of phase variation between them. Their correlation coefficient is −0.417 (exceeding the 99 % confidence level), which indicates that a strong EAWM corresponds to a strong MJO over the equatorial western Pacific. The interannual and interdecadal timescale components of the EAWM and MJO indices can be obtained using a 9-point Gaussian low-pass filter. Their correlation coefficients are −0.466 (exceeding the 99 % confidence level) and −0.242 (exceeding the 90 % confidence level) on interannual and interdecadal timescales, respectively. These results suggest that the relationship between the MJO over the equatorial western Pacific and EAWM on interannual timescales is much stronger than that on interdecadal timescales.

The distribution of correlation coefficients of the 850 hPa MJO kinetic energy with EAWM index is shown in Fig. 2. Areas of negative correlation are concentrated in the equatorial western Pacific west of 160° E with high values over

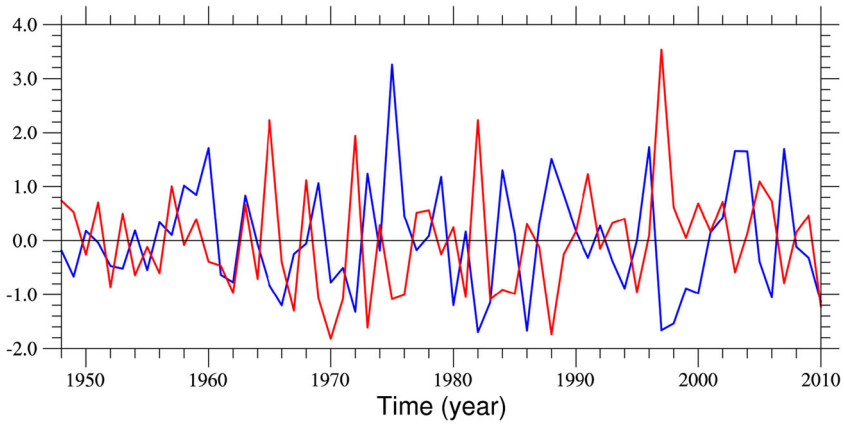


**Fig. 1** The normalized MJO (*blue*) and EAWM (*red*) indices in boreal winter

10° S–10° N, 110°–140° E. However, the MJO near the dateline is positively correlated with the EAWM index, which means the MJO activities there will be weakened in a strong EAWM winter. In addition, the areas with significant correlation are more prominent in the northern hemisphere, whereas the strongest MJO activities are mainly centered in the south of the equator during boreal winter (not shown). A probable explanation is that the MJO over western Pacific has a variety of activity modes, and each has a distinct relationship with the EAWM. Therefore, the influences of the EAWM on each mode differ (discussed below). On the other hand, the mean intertropical convergence zone (ITCZ), South Pacific convergence zone (SPCZ), and ascending branch of Hadley circulation in the boreal winter are located in the southern hemisphere. Thus, although a strong EAWM can enhance the ascending motion and convection north of the equator, the mean background circulation also plays an important role in the southern hemisphere, which causes the main activities center of MJO in the southern hemisphere.

The empirical orthogonal function (EOF) decomposition on the MJO kinetic energy at 850 hPa over western Pacific (15° S–15° N, 115°–165° E) revealed five modes passing the North significant test (North et al. 1982). The first three modes account for 56.88 % of the total variance, and each mode has its own characteristics (Fig. 3). The first mode shows the consistent variation of the MJO over the equatorial western Pacific. The second mode shows the dipole structure of MJO activities in the meridional direction. The third mode primarily shows the tripole structure of MJO activities over the western Pacific.

Table 1 lists the correlation coefficients between the EAWM index and the time series of these three modes on different timescales. The first and third modes are closely related to the EAWM index on raw (unfiltered) and interannual timescales. The first and third modes reflect the consistent and tripole variations of MJO over the western Pacific, respectively, which may explain why the maximum correlation region appears in the area of 10° S–10° N, 110°–140° E (Fig. 2). The first mode is also closely related to the EAWM on interdecadal timescales. Thus, the relationships between the various modes of MJO and EAWM are different, which increases the complexity of the relationships between the EAWM and MJO. As each mode has its own activities and variability characteristics, the relationship between the EAWM and MJO may also be different in different years. For example, the EAWM was strong in 1962/63, 1970/71, and 1983/84 winters, whereas the activities of MJO over the western Pacific were weak. However, there are no strong MJO activities in a weak EAWM winter. That is, there is indeed a certain relationship between the EAWM and MJO, but the impact of the EAWM on the MJO is asymmetric for strong and weak EAWM, and this relationship shows interannual and interdecadal variabilities.

Singular value decomposition (SVD) results (not shown) of the MJO kinetic energy over the western Pacific (20° S–20° N, 110°E–180°) and meridional wind at 850 hPa over the East

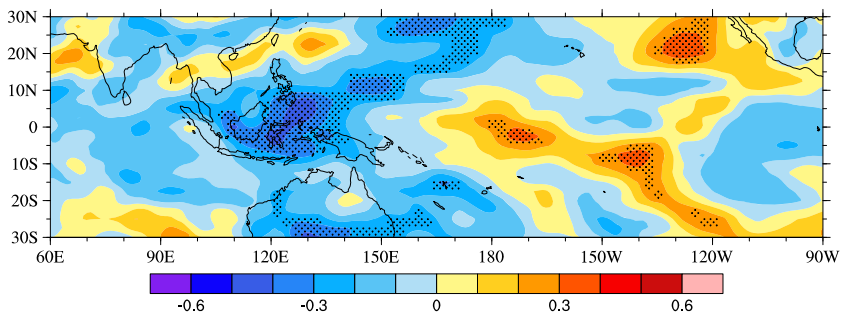


**Fig. 2** Distribution of the correlation coefficients between MJO kinetic energy at 850 hPa and EAWM index. Results passing the significant test at the 90 % confidence level are stippled

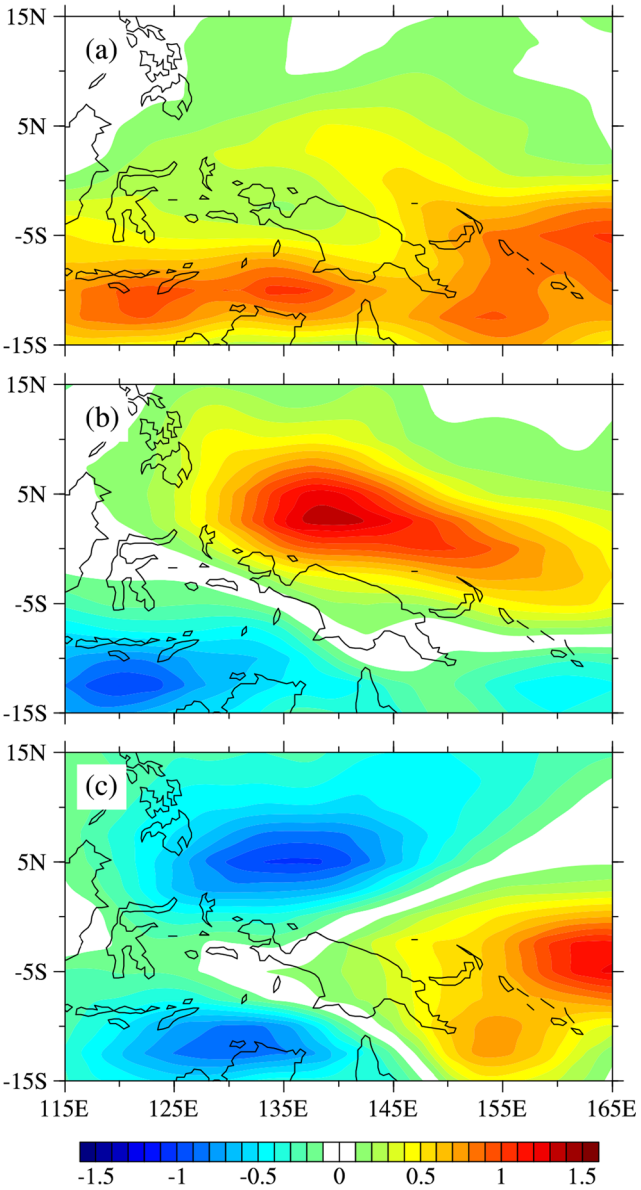


**Fig. 3** Distribution of the **a** first, **b** second, and **c** third EOF modes of MJO kinetic energy ($m^2\ s^{-2}$) at 850 hPa over the tropical western Pacific (15° S–15° N, 115°–165° E)

Asia (10°–40° N, 100°–150° E) in the boreal winter also show that the meridional wind over the East Asian and its neighboring sea is closely related to the MJO over the equatorial western Pacific. These features also suggest a close relationship between the EAWM and MJO, because the strong northerlies at lower troposphere over East Asia in boreal winter can represent a strong EAWM (Wang and Chen 2010).

**Table 1** Correlation coefficients between the EAWM index and the time series of different EOF modes on different timescales. (Results passing the significant test at the 90, 95, and 99 % confidence level are marked with *, **, and ***, respectively)

| | First | Second | Third |
|---|---|---|---|
| Raw data | 0.244* | −0.102 | 0.272** |
| Interannual timescales | 0.231* | −0.145 | 0.355*** |
| Interdecadal timescales | 0.271** | 0.060 | −0.059 |

### 3.2 Composite analysis in anomalous EAWM winters

The above analysis points the out-of-phase variation between EAWM and MJO indices, from which some questions arise. Firstly, is there a prominent difference in the activities of MJO between strong and weak EAWM winters? Furthermore, what is the mechanism of the EAWM influencing the MJO? To address these questions and discuss the influence of anomalous EAWM on the activities of MJO, composite analysis was performed on strong and weak EAWM winters (defined as the amplitude of EAWM index exceeding 0.7 standard deviation). The 18 identified strong EAWM winters are 1952/53, 1962/63, 1964/65, 1967/68, 1969/70, 1970/71, 1971/72, 1973/74, 1975/76, 1976/77, 1981/82, 1983/84, 1984/85, 1985/86, 1988/89, 1995/96, 2007/08, and 2010/11; the 12 identified weak winters are 1948/49, 1951/52, 1957/58, 1965/66, 1968/69, 1972/73, 1982/83, 1991/92, 1997/98, 2002/03, 2005/06, and 2006/2007.

The horizontal distribution of composite MJO kinetic energy and its anomalies at 850 hPa in strong and weak EAWM winters are shown in Fig. 4. In strong EAWM winters, there are two major MJO activity centers over the western Pacific: one is located at 0°–10° N, 120°–150° E and the other is in the southern hemisphere (5°–15° S, 110°–150° E) with their maximum strength exceeding 3.0 and 4.0 $m^2\ s^{-2}$, respectively. The anomalous MJO kinetic energy clearly indicates that the MJO over the western Pacific west of 140° E is enhanced in the strong EAWM winters, whereas it is weakened over the central Pacific (Fig. 4a). However, the activities of MJO have almost opposite characteristics in the weak EAWM winters, featuring reduced/strengthened over the western/central Pacific (Fig. 4b). The activity center in the northern hemisphere is weakened significantly and that in the southern hemisphere is also reduced but not as prominently as the northern center. Moreover, there is a new activity center west of the dateline (10° S, 175° E), with its maximum strength exceeding 3.0 $m^2\ s^{-2}$. The difference of MJO between strong and weak EAWM winters shows that the activities of MJO over the equatorial western Pacific and near the dateline differ significantly between strong and weak EAWM winters, which indicate that EAWM activities have a significant effect on the activities of MJO over these areas.

The activities of MJO are significantly different in strong and weak EAWM winters, but how does the EAWM affect them? The difference of wind and divergence at 850 hPa between strong and weak EAWM winters shows that anomalous westerlies are over the equatorial Indian Ocean and equatorial Pacific west of 150° E, anomalous easterlies are over the

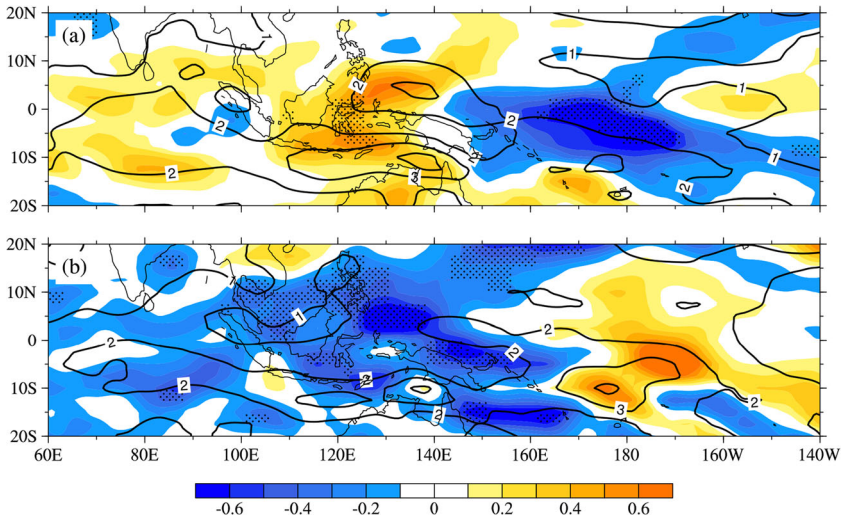


**Fig. 4** Distribution of MJO kinetic energy at 850 hPa (*contours*, $m^2\ s^{-2}$) and its anomalies (*color*, $m^2\ s^{-2}$) in **a** strong and **b** weak EAWM winters. Results passing the significant test at the 90 % confidence level are stippled for anomalies

equatorial Pacific east of 150° E, a strong northerlies are over the eastern China and the South China Sea, and an anomalous cyclonic circulation is present to the east of the Philippines in strong EAWM winters (Fig. 5a). Therefore, the convergence over the equatorial western/eastern Pacific is strengthened/weakened. In the upper troposphere (Fig. 5b), the anomalous circulation and divergence patterns are almost opposite to those at 850 hPa. The equatorial Indian Ocean and equatorial Pacific region west of 160° E is dominated by easterlies anomalies, the region east of 160° E is dominated by westerlies anomalies, and anomalous cyclonic circulation is present in both hemispheres over the central-eastern Pacific. The equatorial western/eastern Pacific shows anomalous divergence/convergence. As the strengthening of convergence, the moisture flux convergence at lower troposphere over the western Pacific is also enhanced in the strong EAWM winters (Fig. 5c). The moisture flux convergence at lower troposphere strengthens significantly over the western Pacific, especially in the northern hemisphere, while it is weakened over the eastern Pacific (Fig. 5c). The anomalous convergence/divergence in the lower/upper troposphere leads to an anomalous ascending motion over the equatorial eastern Indian Ocean and western Pacific from 80° E to 160° E (Fig. 6). The convection over the equatorial western Pacific is also strengthened during the strong EAWM winters, as reflected by the difference of OLR (Fig. 5d). Therefore, the activities of the MJO are enhanced over the equatorial western Pacific, because the feedback effect of convective heating is an important mechanism for the initiation and maintenance of MJO (Li 1985; Lau and Peng 1987; Li et al. 2009).

Based on the above analysis, the EAWM influences the MJO over the equatorial western Pacific mainly through the following processes. First, the northerly surge of the strong EAWM reaches into tropics and strengthens the convection there. Subsequently, the feedback effect of convective heating inspires strong CISK-Rossby waves and CISK-Kelvin waves, which strengthen the activities of MJO (Li 1985; Lau and Peng 1987).

## 4 Impact of EAWM on MJO in its phase 4

The northerlies associated with the strong EAWM can enhance the convection over the equatorial western Pacific and affect the activities of MJO. However, the process of EAWM is discrete pulse-like event, and the MJO activities also have an eastward propagation feature. Wheeler and Hendon (2004) divided the life cycle of the MJO into eight phases according to the location of the active convective center of MJO during its eastward propagation. Therefore, to further study the impact of EAWM on the MJO, we examined strong/weak EAWM processes occurring in the phase 4 of the MJO, in which the convection center of MJO almost locates in the Maritime Continent and the equatorial western Pacific.

A 3-day running mean was firstly applied to the daily EAWM index. The weak EAWM process is defined as the daily EAWM index exceeding 0.8 standard deviation at least for 3 consecutive days, whereas the strong EAWM process is identified if daily EAWM index is smaller than −0.8 standard deviation at least for 3 consecutive days. The first day that exceeds 0.8 standard deviation (or smaller than −0.8 standard deviation) is regarded as day 0 of the process. The strong/weak EAWM processes whose onset date is between November 10 and April 20 were used for the composite, and 19 strong and 11 weak EAWM processes were identified and shown in Table 2.

The evolution of latitudinal distribution of composite anomalous meridional wind at 850 hPa averaged over 110°–130° E in strong and weak EAWM processes is shown in Fig. 7. During the strong EAWM process, East Asia north of 30° N features anomalous northerlies on day −8. On day 0, the strong northerlies of the EAWM reach into the tropics and persist for 6 days. During the weak EAWM process, the

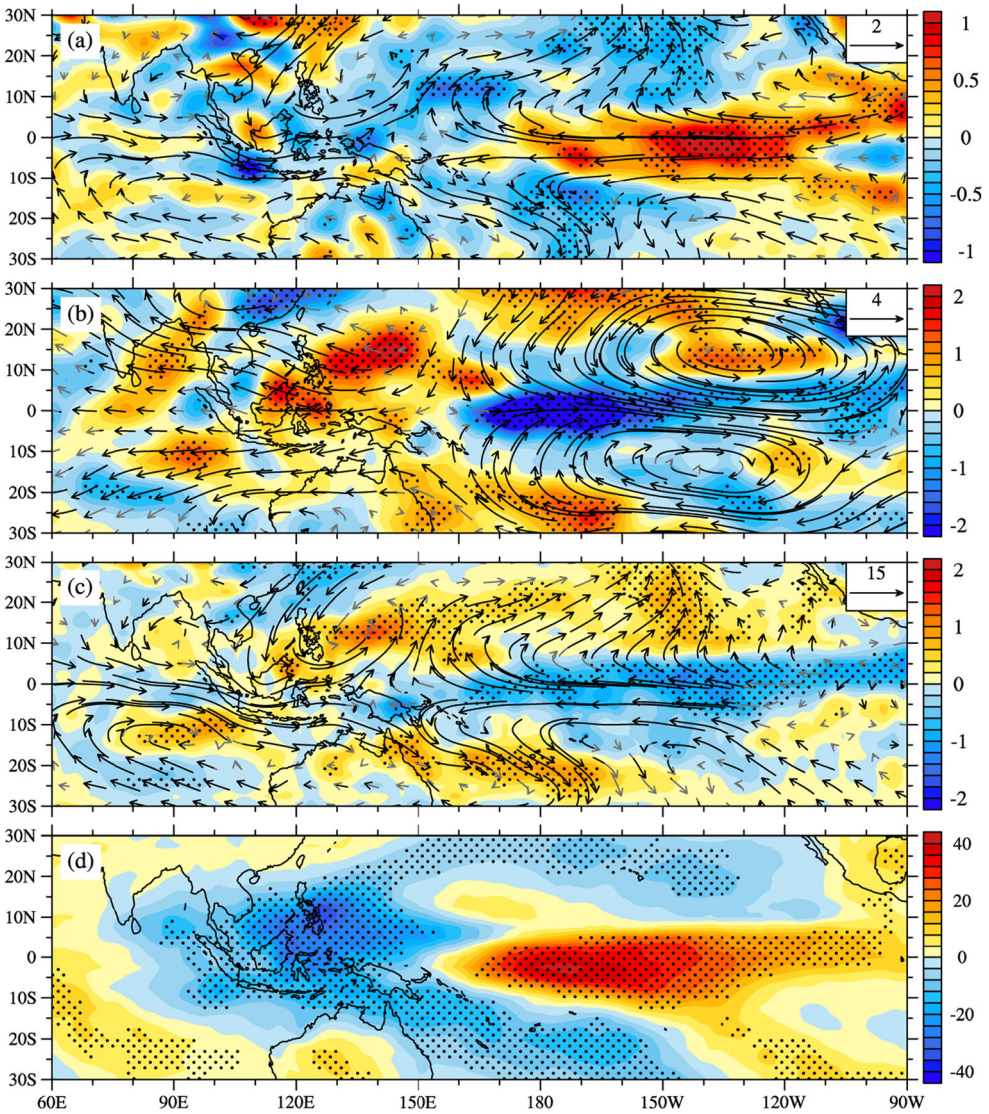


**Fig. 5** Differences of horizontal circulation (*vector*, m $s^{-1}$) and divergence (*color*, $10^{-6}s^{-1}$) at **a** 850 hPa and **b** 200 hPa, **c** moisture flux (*vector*, g $kg^{-1}$ m $s^{-1}$) and its convergence (color, $10^{-5}$g kg $s^{-1}$) averaged from 1000 to 700 hPa, and **d** OLR (W $m^{-2}$) between the strong and weak EAWM winters. Results passing the significant test at the 90 % confidence level are stippled for divergence, moisture flux convergence, and OLR and marked by *black* for wind and moisture flux

anomalous northerlies are active over East Asia before day 0, whereas the strong anomalous southerlies dominate the 110°–130° E region in the tropics on day 0 and persist for 5 days. OLR can reflect the activities of convection in the tropics and widely be used in the studies of MJO (Wheeler and Hendon 2004; Wang et al. 2012). Negative OLR anomalies in the phase 4 of MJO are located mainly in 20° S–20° N, 70°–150° E (not shown), and the large values (<−12 W $m^{-2}$) are

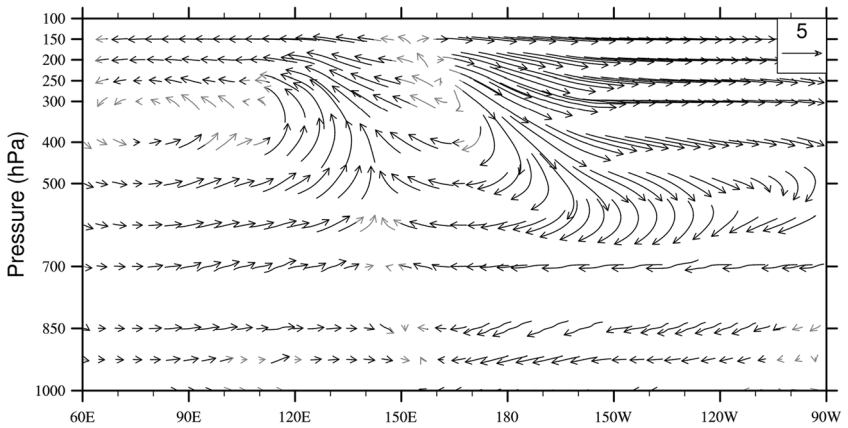


**Fig. 6** Differences of zonal-vertical circulation averaged over 10° S–10° N between strong and weak EAWM winters. Results passing the significant test at the 90 % confidence level are marked by *black*. The vertical velocity is timed by 500

**Table 2** Start and end time of strong and weak EAWM processes

| Strong EAWM | Weak EAWM |
|---|---|
| 1982.01.14–1982.01.18 | 1984.12.13–1984.12.15 |
| 1986.02.19–1986.03.04 | 1992.02.13–1992.02.17 |
| 1987.01.30–1987.02.03 | 1994.12.05–1994.12.11 |
| 1989.04.08–1989.04.10 | 1995.01.19–1995.01.21 |
| 1990.03.03–1990.03.07 | 2000.03.02–2000.03.04 |
| 1991.04.18–1991.04.21 | 2003.02.06–2003.02.08 |
| 1992.02.20–1992.02.24 | 2003.02.26–2003.03.04 |
| 1993.04.04–1993.04.12 | 2003.03.29–2003.04.01 |
| 1994.03.22–1994.03.28 | 2003.11.15–2003.11.19 |
| 1996.01.31–1996.02.09 | 2004.12.01–2004.12.03 |
| 1996.04.01–1996.04.03 | 2005.04.05–2005.04.08 |
| 1997.02.16–1997.02.21 | |
| 2000.02.24–2000.02.26 | |
| 2001.04.09–2001.04.11 | |
| 2001.11.12–2001.11.24 | |
| 2002.11.21–2002.11.24 | |
| 2004.03.04–2004.03.07 | |
| 2008.02.06–2008.02.18 | |
| 2009.11.16–2009.11.20 | |

concentrated mainly in 10° S–10° N, 80°–140° E. Figure 8a, b shows the daily evolution of the equatorially averaged OLR anomalies over 10° S–10° N under strong and weak EAWM processes. There are no prominent differences in the OLR between strong and weak EAWM processes before day 0. However, the OLR is prominently different over Maritime Continent and western Pacific (especially over the western Pacific) after day 0. On the one hand, the convection is suppressed after day 0 under the weak EAWM process; in contrast, it becomes more active under the strong EAWM process. These differences are more prominent over the western Pacific, which means that the EAWM has a stronger impact on the convection there. The convection reaches its maximum near day 5 in the strong EAWM process, which is consistent with the disappearance of strong EAWM on day 5 (Fig. 7a). On the other hand, the eastward propagation of OLR is more persistent and prominent under the strong EAWM process; in contrast, it is discontinued under the weak EAWM process. The zonal wind and kinetic energy of MJO at 850 hPa also show similar characteristics (not shown), which suggests that the EAWM not only influence the intensity of MJO but also impact its eastward propagation over the equatorial Pacific.

The composite results of the vertically averaged (1000–700 hPa) moisture flux convergence averaged over 10° S–10° N (Fig. 8c, d) clearly show that under the strong EAWM process, the moisture flux convergence is strengthened after day 0 over the Maritime Continent and western Pacific. In contrast, the moisture flux convergence is weakened after day 0 under the weak EAWM process there. Further exploration shows that the strengthening of moisture flux convergence over the western Pacific after day 0 under strong EAWM process (Fig. 8c) mainly due to the meridional component of moisture flux convergence (Fig. 8g), whereas the meridional component (Fig. 8h) reduces the moisture flux convergence under weak EAWM process (Fig. 8d). The zonal component of moisture flux convergence has a contribution to the moisture flux convergence around 120° E after day 0 under weak EAWM process (Fig. 8f), but the negative anomalies of meridional component of moisture flux convergence are stronger (Fig. 8h), which leads to the decrease of horizontal moisture flux convergence under weak EAWM process (Fig. 8d).

Convection is always accompanied by the ascending motion. The evolution of averaged (10° S–10° N, 120°–150° E) anomalous vertical velocity (Fig. 9a, b) clearly shows that the anomalous vertical velocity over the equatorial western Pacific is dominated by descending motion before day −5, which gradually converts into ascending motion after day −5 under strong EAWM process. This strong anomalous ascending motion can persist to day 10. However, under weak EAWM process (Fig. 9b), the anomalous ascending motion is weakened rapidly after day 0, although it is stronger before day 0.

Moist static energy is a good indicator of MJO activities and has been widely used in the studies of MJO (Kemball-Cook and Weare 2001; Wang et al. 2012). The evolution of the averaged (10° S–10° N, 120°–150° E) anomalous moist static energy (Fig. 9c, d) clearly shows that it gradually increases

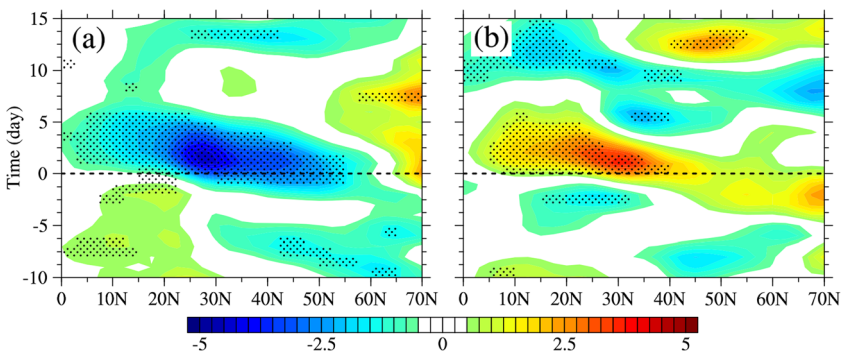


**Fig. 7** Evolution of latitudinal distributions of anomalous meridional wind (m $s^{-1}$) at 850 hPa averaged over 110°–130° E in **a** strong and **b** weak EAWM processes. Negative (positive) in time coordinate indicates before (after) the onset of EAWM. Results passing the significant test at the 90 % confidence level are stippled

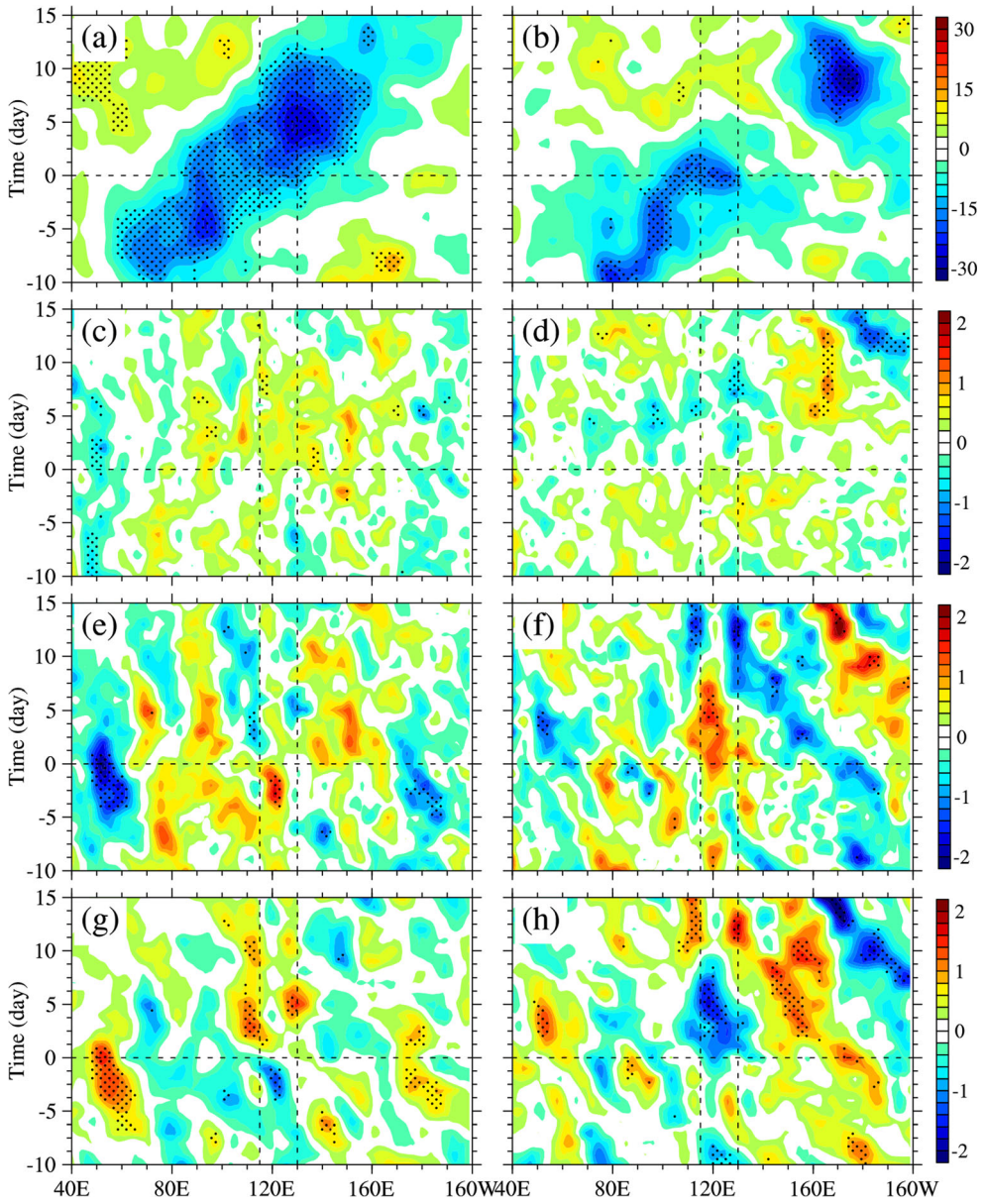


**Fig. 8** **a–h** Evolution of longitudinal distribution of anomalous (from *top* to *bottom*) OLR (W $m^{-2}$), horizontal moisture flux convergence ($10^{-5}$ g $kg^{-1}$m $s^{-1}$) averaged from 1000 to 700 hPa and its zonal and meridional components averaged over 10° S–10° N in (*left column*) strong and (*right*) weak EAWM processes. Results passing the significant test at the 90 % confidence level are stippled. The two *vertical dotted lines* represent the west and east boundaries of the area used to define the EAWM index

after day −3 and reaches its maximum near day 5 under strong EAWM process, which is consisted with the maximum of anomalous northerly and OLR (Figs. 7a and 8a). Under weak EAWM process, however, the moist static energy gradually decreases after day 0, although it is very strong between day −5 and day 0. A strong EAWM can clearly enhance the moist static energy over the equatorial western Pacific, which also reflects the strong activities of MJO under strong EAWM process. The EAWM can also influence the stability of the atmosphere over the western Pacific. The atmospheric instability index (Fig. 10) defined by Kemball-Cook and Weare (2001) as the difference of moist static energy between 1000 and 500 hPa shows that the atmosphere is unstable from day 2 to day 10 under strong EAWM process, but it is almost stable under the weak EAWM process. The instability of atmosphere is favor to the activities of convection and also to the activities of MJO.

Above analysis shows that the physical quantities, such as MJO kinetic energy, convection, moisture flux convergence, moist static energy, and atmospheric stability, differ significantly between strong and weak EAWM processes. And these differences can lead to the anomalies of MJO intensity and propagation.

## 5 Summary and discussion

The activities of MJO and their anomalies are the frontier scientific issues receiving broad attentions. The equatorial western Pacific is one of the primary activities areas of

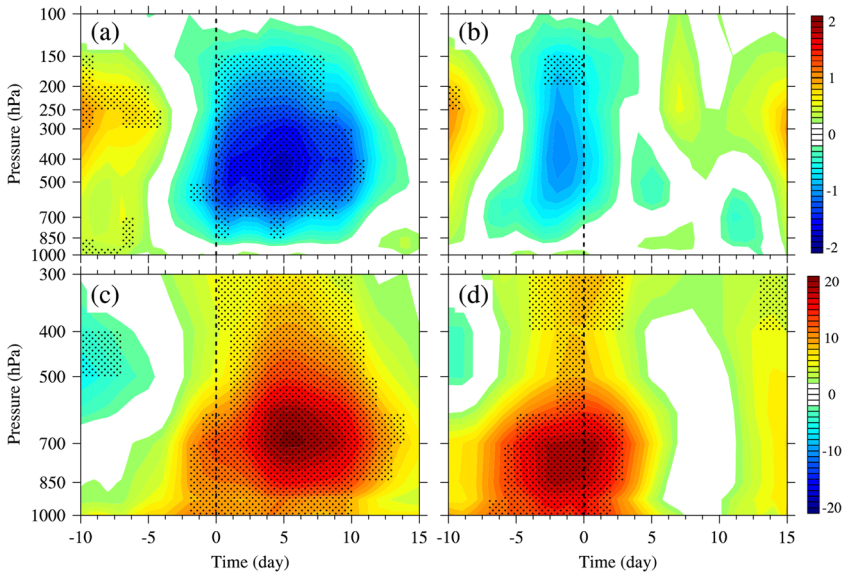


**Fig. 9** **a–d** Evolution of vertical distribution of anomalous (*top panel*) vertical velocity ($10^{-2}$Pa $s^{-1}$) and (*bottom*) moist static energy ($10^3$ J $kg^{-1}$) averaged over 10° S–10° N, 120°–150° E in (*left column*) strong and (*right*) weak EAWM processes. Results passing the significant test at the 90 % confidence level are stippled

MJO. This study has investigated the relationship between the EAWM and MJO over the equatorial western Pacific using reanalysis data, and the main conclusions are as follows:

Both the EAWM and MJO over the equatorial western Pacific have significant interannual and interdecadal variabilities, and they are related significantly, especially on the interannual timescales. The processes by which the EAWM reinforces the MJO over the western Pacific are due to the northerlies associated with strong EAWM intruding into equatorial regions and leading to a strengthened convection over the equatorial western Pacific. Based on feedback effect of convective heating, the strengthened convection can generate a stronger MJO. The relationship between the MJO and EAWM is unstable and shows interannual and interdecadal variabilities. One possible explanation for these variabilities is that the MJO activities over the western Pacific have different modes, and the relationship between each mode and the EAWM differ.

The composite analysis in the phase 4 of the MJO shows that the MJO kinetic energy, convection, moisture flux convergence, vertical velocity, zonal wind at 850 hPa, moist static energy, atmospheric stability, and other physical quantities over the Maritime Continent and western Pacific all differ significantly between strong and weak EAWM processes. The generation and evolution of these differences are directly linked to the intrusion of strong northerlies associated with the strong EAWM into the tropics. The strong EAWM not only enhances the intensity of MJO over the equatorial western Pacific but can also lead to the eastward propagation of MJO more persistent over the equatorial Pacific.

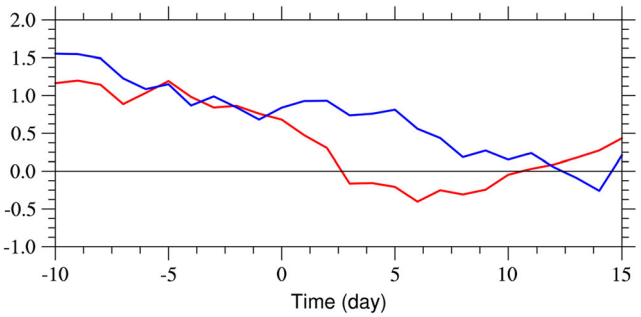


**Fig. 10** The atmospheric instability index ($10^3$ J $kg^{-1}$) in strong (*red*) and weak (*blue*) EAWM processes averaged over 10° S–10° N, 120°–150° E

The EAWM has a reinforcing effect on the MJO over the Maritime Continent and equatorial western Pacific, but this effect can also be modified by other factors, such as the influence of the southern hemisphere systems, the distribution of anomalous convective heating profiles caused by the EAWM and so on. Therefore, the EAWM is an important factor that affects the activities of MJO over the Maritime Continent and western Pacific, but it is not the only factor, which also leads to the interannual and interdecadal variabilities in the relationship between the EAWM and MJO.

Some simple numerical experiments about the EAWM exciting the activities of convection over tropical western Pacific has been done, but more numerical simulation studies for the results revealed by this paper using a high-resolution mode will be the following work.

**Acknowledgments** This research is sponsored by the National Basic Research Program of China (Grant No. 2015CB453200, 2013CB956200) and National Nature Science Foundation of China (Grant No., 41475070, 41575062, 41520104008).

## References

Chan JCL, Li CY (2004) The East Asian winter monsoon, East Asian Monsoon, CP Chang Ed., World Scientific Publisher, Singapore 54–106

Chang CP, Erickson JE, Lau KM (1979) Northeasterly cold surges and near-equatorial disturbances over the winter MONEX area during December 1974. Part I: synoptic aspects. Mon Weather Rev 107: 812–829

Chen W, Yang S, Huang RH (2005) Relationship between stationary planetary wave activity and the East Asian winter monsoon. J Geophys Res 110:D14. doi:10.1029/2004JD005669

Duchon CE (1979) Lanczos filtering in one and two dimensions. J Appl Meteorol 18:1016–1022

Hendon HH, Wheeler MC, Zhang C (2007) Seasonal dependence of the MJO–ENSO relationship. J Clim 20:531–543

Hsu HH, Hoskins BJ, Jin FF (1990) The 1985/86 intraseasonal oscillation and the role of the extratropics. J Atmos Sci 47:823–839

Huang RH, Zhou LT, Chen W (2003) The progresses of recent studies on the variabilities of the East Asian monsoon and their causes. Adv Atmos Sci 20:55–69

Huang RH, Chen JL, Huang G (2007a) Characteristics and variations of the East Asian monsoon system and its impact on climate disasters in China. Adv Atmos Sci 24(6):993–1023. doi:10.1007/s00376-007-0993-x

Huang RH, Wei K, Chen JL, Chen W (2007b) The East Asian winter monsoon anomalies in the winters of 2005 and 2006 and their relations to the quasi-stationary planetary wave activity in the Northern Hemisphere (in Chinese). Chinese J Atmos Sci 31(6):1033–1048

Ji LR, Sun SQ, Arpe K, Bengisson L (1997) Model study on the interannual variability of Asian winter monsoon and its influence. Adv Atmos Sci 14(1):1–22

Kalnay E, Kanamitsu M, Kistler R, Collins W, Deaven D, Gandin L, Iredell M, Saha S, White G, Woollen J, Zhu Y, Chelliah M, Ebisuzaki W, Higgins W, Janowiak J, Mo KC, Ropelewski C, Wang J, Leetma A, Reynolds R, Jenne R, Joseph D (1996) The NCEP/NCAR 40-year reanalysis project. Bull Am Met Soc 77: 437–471

Kemball-Cook SR, Weare BC (2001) The onset of convection in the Madden-Julian oscillation. J Clim 14:780–793

Lau KM, Peng L (1987) Origin of low-frequency (intraseasonal) oscillations in the tropical atmosphere. Part I: basic theory. J Atmos Sci 44: 950–972

Li CY (1985) Actions of summer monsoon troughs (ridges) and tropical cyclone over South Asia and the moving CISK mode. Scientia China (B) 28:1197–1206

Li CY (1989) Frequent activities of stronger aerotroughs in East Asia in wintertime and the occurrence of the El Nino event. Sci China (B) 32:976–985

Li CY, Mu MQ (2000) Relationship between East-Asian winter monsoon, warm pool situation and ENSO cycle (in Chinese). Chin Sci Bull 45:1448–1455

Li CY, Zhou YP (1994) Relationship between intraseasonal oscillation in the tropical atmosphere and ENSO (in Chinese). Chinese J Geophysics 37:213–223

Li RCY, Zhou W (2013a) Modulation of western north Pacific tropical cyclone activity by the ISO. Part I: genesis and intensity. J Clim 26: 2904–2918

Li RCY, Zhou W (2013b) Modulation of western north Pacific tropical cyclone activity by the ISO. Part II: tracks and landfalls. J Clim 26: 2919–2930

Li CY, Jia XL, Ling J, Zhou W, Zhang CD (2009) Sensitivity of MJO simulations to diabatic heating profiles. Climate Dyn 32:167–187

Li RCY, Zhou W, Chan JCL (2012) Asymmetric modulation of western north Pacific cyclogenesis by the Madden-Julian oscillation under ENSO conditions. J Clim 25:5374–5385

Li CY, Ling J, Song J, Pan J, Tian H, Chen X (2014) Research progress in China on the tropical atmospheric intraseasonal oscillation. J Meteorol Res 28:671–692

Liebmann B, Hartmann DL (1984) An observational study of tropical-midlatitude interaction on intraseasonal time scales during winter. J Atmos Sci 41(23):3333–3350

Liebmann B, Smith CA (1996) Description of a complete (interpolated) outgoing longwave radiation dataset. Bull Am Met Soc 77:1275–1277

Ling J, Zhang C, Bechtold P (2013) Large-scale distinctions between MJO and Non-MJO convective initiation over the tropical Indian Ocean. J Atmos Sci 70:2696–2712

Ling J, Li CY, Zhou W, Jia XL (2014) To begin or not to begin? A case study on the MJO initiation problem. Theor Appl Climatol 115:231–241

Lü JM, Jü JH, Ren JZ, Gan WW (2012) The influence of the Madden-Julian oscillation activity anomalies on Yunnan's extreme drought of 2009–2010. Sci China Earth Sci 55:98–112. doi:10.1007/s11430-011-4348-1

Madden RA, Julian PR (1971) Detection of a 40–50 day oscillation in the zonal wind in the tropical Pacific. J Atmos Sci 28:702–708

Madden RA, Julian PR (1972) Description of global scale circulation cells in the tropics with 40–50 day period. J Atmos Sci 29:1109–1123

Madden RA, Julian PR (1994) Observations of the 40–50-day tropical oscillation—A review. Mon Weather Rev 122:814–837

Murakami T (1988) Intraseasonal atmospheric teleconnection patterns during the Northern Hemisphere winter. J Clim 1(2):117–131

North GR, Bell T, Cahalan R, Moeng FJ (1982) Sampling errors in the estimation of empirical orthogonal function. Mon Weather Rev 110: 699–706

Pan J, Li CY, Song J (2010) The modulation of Madden-Julian oscillation on typhoons in the northwestern Pacific Ocean (in Chinese). Chinese J Atmos Sci 34(6):1059–1070

Ray P, Zhang C (2010) A case study of the mechanics of extratropical influence on the initiation of the Madden–Julian oscillation. J Atmos Sci 67:515–528. doi:10.1175/2009JAS3059.1

Ray P, Zhang C, Dudhia J, Chen SS (2009) A numerical case study on the initiation of the Madden–Julian oscillation. J Atmos Sci 66:310–331. doi:10.1175/2008JAS2701.1

Wang L, Chen W (2010) How well do existing indices measure the strength of the East Asian winter monsoon? Adv Atmos Sci 27: 855–870

Wang ZY, Ding YH (2006) Climate change of the cold wave frequency of China in the last 53 years and the possible reasons (in Chinese). Chinese J Atmos Sci 30(6):1068–1076

Wang L, Huang RH, Gu L, Chen W, Kang LH (2009) Interdecadal variations of the East Asian winter monsoon and their association with quasi-stationary planetary wave activity. J Clim 22:4860–4872

Wang L, Kodera K, Chen W (2012) Observed triggering of tropical convection by a cold surge: implications for MJO initiation. Quart J R Meteorol Soc 138(668):1740–1750. doi:10.1002/qj.1905

Wheeler MC, Hendon HH (2004) An all-season real-time multivariate MJO index: development of an index for monitoring and prediction. Mon Weather Rev 132(8):1917–1932

Yan HM, Zhou W, Yang H, Cai Y (2009) Definition of an East Asian winter monsoon index and its variation characteristics (in Chinese). Trans Atmos Sci 32(3):367–376

Yang H, Li CY (2003) The relation between atmospheric intraseasonal oscillation and summer severe flood and drought in the Changjiang-Huaihe river basin. Adv Atmos Sci 20(4):540–553

Zhang CD (2005) Madden-Julian oscillation. Rev Geophy 43:RG2003. doi:10.1029/2004RG000158

Zhang CD (2013) Madden-Julian oscillation: bridging weather and climate. Bull Am Meteorol Soc 94:1849–1870. doi:10.1175/BAMS-D-12-00026.1

Zhang CD, Gottschalck J (2002) SST anomalies of ENSO and the Madden-Julian oscillation in the equatorial Pacific. J Clim 15: 2429–2445

Zhou LT (2011) Impact of East Asian winter monsoon on rainfall over southeastern China and its dynamical process. Int J Climatol 31(5): 677–686. doi:10.1002/joc.2101

Zhou W, Chan JCL (2005) Intraseasonal oscillations and the South China Sea summer monsoon onset. Int J Climatol 25(12): 1585–1609

Zhou W, Wang X, Zhou TJ, Li C, Chan JCL (2007) Interdecadal variability of the relationship between the East Asian winter monsoon and ENSO. Meteor Atmos Phys 98:283–229

Zhu CW, Nakazawa T, Li JP (2004) Modulation of tropical depression/cyclone over the Indian-western Pacific oceans by Madden-Julian oscillation (in Chinese). Acta Meteorologica Sinca 62(1):42–50